

Observation of $\bar{B}^0 \rightarrow D^0 \pi^0$ and $\bar{B}^0 \rightarrow D^{*0} \pi^0$

(CLEO Collaboration)

(January 11, 2002)

Abstract

We have studied the color-suppressed hadronic decays of neutral B mesons into the final states $D^{(*)0} \pi^0$. Using 9.67 million $B\bar{B}$ pairs collected with the CLEO detector, we observe the decays $\bar{B}^0 \rightarrow D^0 \pi^0$ and $\bar{B}^0 \rightarrow D^{*0} \pi^0$ with the branching fractions $\mathcal{B}(\bar{B}^0 \rightarrow D^0 \pi^0) = (2.74_{-0.32}^{+0.36} \pm 0.55) \times 10^{-4}$ and $\mathcal{B}(\bar{B}^0 \rightarrow D^{*0} \pi^0) = (2.20_{-0.52}^{+0.59} \pm 0.79) \times 10^{-4}$. The first error is statistical and the second systematic. The statistical significance of the $D^0 \pi^0$ signal is 12.1σ (5.9σ for $D^{*0} \pi^0$). Utilizing the $\bar{B}^0 \rightarrow D^{(*)0} \pi^0$ branching fractions we determine the strong phases $\delta_{I,D^{(*)}}$ between isospin 1/2 and 3/2 amplitudes in the $D\pi$ and $D^*\pi$ final states to be $\cos \delta_{I,D} = 0.89 \pm 0.08$ and $\cos \delta_{I,D^*} = 0.89 \pm 0.08$, respectively.

T. E. Coan,¹ Y. S. Gao,¹ F. Liu,¹ Y. Maravin,¹ I. Narsky,¹ R. Stroynowski,¹ J. Ye,¹ M. Artuso,² C. Boulahouache,² K. Bukin,² E. Dambasuren,² R. Mountain,² T. Skwarnicki,² S. Stone,² J.C. Wang,² A. H. Mahmood,³ S. E. Csorna,⁴ I. Danko,⁴ Z. Xu,⁴ G. Bonvicini,⁵ D. Cinabro,⁵ M. Dubrovin,⁵ S. McGee,⁵ A. Bornheim,⁶ E. Lipeles,⁶ S. P. Pappas,⁶ A. Shapiro,⁶ W. M. Sun,⁶ A. J. Weinstein,⁶ G. Masek,⁷ H. P. Paar,⁷ R. Mahapatra,⁸ R. J. Morrison,⁸ H. N. Nelson,⁸ R. A. Briere,⁹ G. P. Chen,⁹ T. Ferguson,⁹ G. Tatishvili,⁹ H. Vogel,⁹ N. E. Adam,¹⁰ J. P. Alexander,¹⁰ C. Bebek,¹⁰ K. Berkelman,¹⁰ F. Blanc,¹⁰ V. Boisvert,¹⁰ D. G. Cassel,¹⁰ P. S. Drell,¹⁰ J. E. Duboscq,¹⁰ K. M. Ecklund,¹⁰ R. Ehrlich,¹⁰ L. Gibbons,¹⁰ B. Gittelman,¹⁰ S. W. Gray,¹⁰ D. L. Hartill,¹⁰ B. K. Heltsley,¹⁰ L. Hsu,¹⁰ C. D. Jones,¹⁰ J. Kandaswamy,¹⁰ D. L. Kreinick,¹⁰ A. Magerkurth,¹⁰ H. Mahlke-Krüger,¹⁰ T. O. Meyer,¹⁰ N. B. Mistry,¹⁰ E. Nordberg,¹⁰ M. Palmer,¹⁰ J. R. Patterson,¹⁰ D. Peterson,¹⁰ J. Pivarski,¹⁰ D. Riley,¹⁰ A. J. Sadoff,¹⁰ H. Schwarthoff,¹⁰ M. R. Shepherd,¹⁰ J. G. Thayer,¹⁰ D. Urner,¹⁰ B. Valant-Spaight,¹⁰ G. Viehhauser,¹⁰ A. Warburton,¹⁰ M. Weinberger,¹⁰ S. B. Athar,¹¹ P. Avery,¹¹ C. Prescott,¹¹ H. Stoeck,¹¹ J. Yelton,¹¹ G. Brandenburg,¹² A. Ershov,¹² D. Y.-J. Kim,¹² R. Wilson,¹² K. Benslama,¹³ B. I. Eisenstein,¹³ J. Ernst,¹³ G. D. Gollin,¹³ R. M. Hans,¹³ I. Karliner,¹³ N. Lowrey,¹³ M. A. Marsh,¹³ C. Plager,¹³ C. Sedlack,¹³ M. Selen,¹³ J. J. Thaler,¹³ J. Williams,¹³ K. W. Edwards,¹⁴ R. Ammar,¹⁵ D. Besson,¹⁵ X. Zhao,¹⁵ S. Anderson,¹⁶ V. V. Frolov,¹⁶ Y. Kubota,¹⁶ S. J. Lee,¹⁶ S. Z. Li,¹⁶ R. Poling,¹⁶ A. Smith,¹⁶ C. J. Stepaniak,¹⁶ J. Urheim,¹⁶ S. Ahmed,¹⁷ M. S. Alam,¹⁷ L. Jian,¹⁷ M. Saleem,¹⁷ F. Wappler,¹⁷ E. Eckhart,¹⁸ K. K. Gan,¹⁸ C. Gwon,¹⁸ T. Hart,¹⁸ K. Honscheid,¹⁸ D. Hufnagel,¹⁸ H. Kagan,¹⁸ R. Kass,¹⁸ T. K. Pedlar,¹⁸ J. B. Thayer,¹⁸ E. von Toerne,¹⁸ M. M. Zoeller,¹⁸ S. J. Richichi,¹⁹ H. Severini,¹⁹ P. Skubic,¹⁹ S.A. Dytman,²⁰ S. Nam,²⁰ V. Savinov,²⁰ S. Chen,²¹ J. W. Hinson,²¹ J. Lee,²¹ D. H. Miller,²¹ V. Pavlunin,²¹ E. I. Shibata,²¹ I. P. J. Shipsey,²¹ D. Cronin-Hennessy,²² A.L. Lyon,²² C. S. Park,²² W. Park,²² and E. H. Thorndike²²

¹Southern Methodist University, Dallas, Texas 75275

²Syracuse University, Syracuse, New York 13244

³University of Texas - Pan American, Edinburg, Texas 78539

⁴Vanderbilt University, Nashville, Tennessee 37235

⁵Wayne State University, Detroit, Michigan 48202

⁶California Institute of Technology, Pasadena, California 91125

⁷University of California, San Diego, La Jolla, California 92093

⁸University of California, Santa Barbara, California 93106

⁹Carnegie Mellon University, Pittsburgh, Pennsylvania 15213

¹⁰Cornell University, Ithaca, New York 14853

¹¹University of Florida, Gainesville, Florida 32611

¹²Harvard University, Cambridge, Massachusetts 02138

¹³University of Illinois, Urbana-Champaign, Illinois 61801

¹⁴Carleton University, Ottawa, Ontario, Canada K1S 5B6

and the Institute of Particle Physics, Canada

¹⁵University of Kansas, Lawrence, Kansas 66045

¹⁶University of Minnesota, Minneapolis, Minnesota 55455

¹⁷State University of New York at Albany, Albany, New York 12222

¹⁸Ohio State University, Columbus, Ohio 43210

- ¹⁹University of Oklahoma, Norman, Oklahoma 73019
- ²⁰University of Pittsburgh, Pittsburgh, Pennsylvania 15260
- ²¹Purdue University, West Lafayette, Indiana 47907
- ²²University of Rochester, Rochester, New York 14627

The decay $\bar{B}^0 \rightarrow D^{(*)0} \pi^0$ proceeds predominantly through the internal spectator diagram shown in Fig. 1. This diagram is color-suppressed, since the color of the quark-pair originating from the W decay must match the color of the other quark pair. The rate of $\bar{B}^0 \rightarrow D^{(*)0} \pi^0$ relative to $B^- \rightarrow D^{(*)0} \pi^-$ is suppressed, crudely, by one factor of $(1/3)^2$, and an additional $(1/\sqrt{2})^2$ due to the projection of the $d\bar{d}$ state onto the pion wave function [1]. This gives a total suppression of 1/18 compared to the color-favored decay modes. Detailed theoretical calculations [2] predict an even larger suppression of about a factor 1/50.

So far the only established color-suppressed decays are two-body B decays into Charmonium plus neutral hadrons. A measurement of $\bar{B}^0 \rightarrow D^{(*)0} \pi^0$ is therefore a benchmark test for theoretical models of hadronic B decays [1,2]. An investigation of color-suppressed decays into a D meson and light neutral mesons other than a π^0 is currently underway and will be addressed in a future publication.

The observation of $\bar{B}^0 \rightarrow D^{(*)0} \pi^0$ completes the measurement of $D^{(*)} \pi$ final states and allows us to extract the strong phase difference between isospin 1/2 and 3/2 amplitudes [2,3].

In this Letter we present the observation of $\bar{B}^0 \rightarrow D^{(*)0} \pi^0$, superseding the limits from our previous publication [4]. Our new analysis has significantly increased statistics and is based on a data sample with improved calibration and track reconstruction. The background shapes and the signal separation power have also been significantly improved. Charge conjugates are implied throughout the paper. Our analysis uses e^+e^- annihilation data recorded with the CLEO detector at the Cornell Electron Storage Ring. The integrated luminosity of our data sample is 9.15 fb^{-1} for data collected on the $\Upsilon(4S)$ (on-resonance), corresponding to 9.67 million $B\bar{B}$ pairs, and 4.35 fb^{-1} collected 60 MeV below the $B\bar{B}$ threshold (off-resonance), which is used for background studies.

CLEO is a general purpose solenoidal magnet detector. Data were recorded with two detector configurations, CLEO II and CLEO II.V [5,6]. Cylindrical drift chambers in a 1.5T solenoidal magnetic field measure momentum and specific ionization (dE/dx) of charged particles. Photons are detected using a CsI(Tl) crystal electromagnetic calorimeter, consisting of a barrel-shaped central part of 6144 crystals and 1656 crystals in the forward regions of the detector (endcaps). In the II.V configuration the innermost chamber was replaced by a three-layer, double-sided silicon microvertex detector, and the main drift chamber gas was changed from argon-ethane to a helium-propane mixture. As a result of these modifications, the CLEO II.V part of the data (2/3 of the total sample) has improved momentum resolution and particle identification.

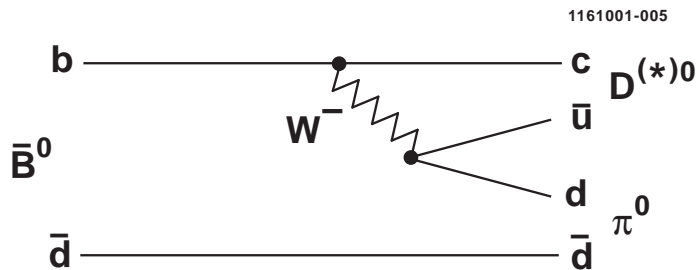


FIG. 1. Diagram for the color-suppressed decay $\bar{B}^0 \rightarrow D^{(*)0} \pi^0$.

B mesons were reconstructed by selecting high-momentum $D^{(*)0}$ and π^0 mesons. Track quality requirements are imposed on charged tracks and the purity of pion and kaons is improved by using dE/dx information whenever available. The π^0 candidates are reconstructed from isolated electromagnetic clusters of at least 30 MeV in the barrel region and 50 MeV in the endcaps. The mass resolution is 8 MeV in the barrel region and 10 MeV in the endcaps. We require that the candidate's mass is within 2.5 standard deviations (σ) of the nominal π^0 mass. Prompt π^0 's from B decays are required to have a momentum larger than 1.8 GeV.

D^0 mesons are selected in the decay modes $D^0 \rightarrow K^- \pi^+$, $D^0 \rightarrow K^- \pi^+ \pi^0$ and $D^0 \rightarrow K^- \pi^+ \pi^+ \pi^-$. The invariant mass of the D daughter particles is required to be within 2.5 σ of the known D^0 mass. The mass resolution depends on the decay mode and is between 6 and 12 MeV. The momentum of the D^0 is required to be larger than 1.65 GeV. In the $D^0 \rightarrow K^- \pi^+ \pi^0$ mode we suppress combinatorial background by using only certain regions of the Dalitz plane.

D^{*0} mesons are selected in the decay modes $D^{*0} \rightarrow D^0 \pi^0$ and $D^{*0} \rightarrow D^0 \gamma$. To reduce the combinatorial background in the decay mode $D^{*0} \rightarrow D^0 \gamma$ we require that the D^0 decays into $K^- \pi^+$. We require that the mass difference $m_{D^{*0}} - m_{D^0}$ is within 2.5σ of the known value and that the momentum of the D^{*0} is larger than 1.8 GeV. The kinematic resolution of π^0 and $D^{(*)0}$ candidates is improved by a mass-constrained kinematic fit.

B decay candidates are selected from π^0 and $D^{(*)0}$ pairings that have no electromagnetic clusters in common. B candidates are identified using a beam-constrained mass $M_B = \sqrt{E_{\text{beam}}^2 - p_B^2}$, where E_{beam} is the beam energy and p_B is the B candidate momentum, and an energy difference $\Delta E = E_D + E_{\pi^0} - E_{\text{beam}}$, where E_D and E_{π^0} are the energies of the $D^{(*)0}$ and π^0 . The resolution in M_B depends on the D decay mode and is between 3.5 and 4 MeV. The resolution is dominated by the beam energy spread and the π^0 energy resolution. The resolution in ΔE is between 35 and 40 MeV. The energy resolution is slightly asymmetric due to the energy loss out of the back of the CsI crystals. The mass-constrained kinematic fit to the pion 4-momentum compensates for most of this effect. We accept B candidates with M_B above 5.24 GeV and $|\Delta E| < 300$ MeV. To better suppress background from $e^+e^- \rightarrow q\bar{q}$ events (continuum background), several event shape variables are combined into a Fisher discriminant \mathcal{F}_D [7]. For $B\bar{B}$ events (continuum background), the \mathcal{F}_D distribution is almost a Gaussian and has its maximum at 0.42 (0.57). The standard deviation is 0.11 (0.12). The separation between the $B\bar{B}$ and continuum distributions is 1.3 σ . We reject clear continuum events by requiring $\mathcal{F}_D < 1$. For each candidate we calculate the sphericity vectors [8] of the B daughter particles and of the rest of the event. We require the cosine of the angle between these two vectors to be within -0.8 and 0.8. The distribution of this angle is strongly peaked at ± 1 for continuum background and is nearly flat for $B\bar{B}$ events.

The number of signal events in the sample is obtained from unbinned, extended maximum likelihood fits. The free parameters of the fits are the number of signal events, background from B decays ($B\bar{B}$) and from continuum e^+e^- annihilation (continuum). Four variables are used as input to the maximum likelihood fit: the beam-constrained mass M_B , the energy difference ΔE , the Fisher Discriminant \mathcal{F}_D , and the cosine of the decay angle of the B $\cos \theta_{\text{BHel}}$, defined as the angle between the $D^{(*)}$ momentum and the B flight direction calculated in the B rest frame.

In each of the fits, the likelihood of the B candidate is the sum of probabilities for the

signal and two background hypotheses with relative weights maximizing the likelihood. The probability of a particular hypothesis is the product of probability density functions (PDFs) for each of the input variables. The PDFs for M_B are represented by a bifurcated Gaussian [9] for signal, an empirical shape, $M_B \sqrt{(1-x^2)} \exp(-E_{fact}(1-x^2))$, with $x = M_B/E_{beam}$, for continuum and a Gaussian on top of the empirical background shape¹ for $B\bar{B}$; the PDFs for ΔE are the sum of two Gaussians with a common mean (signal), 1st-order polynomial (continuum) and a sum of two Gaussians plus a 1st-order polynomial ($B\bar{B}$); the PDFs for \mathcal{F}_D are the sum of two Gaussians with a common mean; and the PDFs for $\cos\theta_{BHel.}$ are 2nd-order polynomials. The PDF parameters are determined from off-resonance CLEO data (continuum) and from high-statistics Monte-Carlo (MC) samples (signal and $B\bar{B}$).

Monte Carlo experiments are generated to test the fitting procedure and to obtain the relation between fit yield and signal branching fractions. The experiments are repeated several hundred times with different Monte Carlo test samples randomly selected from high-statistics MC samples.

We summarize the results of the fits to CLEO data in Table I. We give results for all B decay modes, corresponding D decay modes and the combination of all D decay modes. We combine the results for different D decay modes by adding the log likelihood as a function of the branching fraction. Branching fractions for each mode are obtained via

$$\mathcal{B}(\bar{B}^0 \rightarrow D^{(*)0} \pi^0) = \frac{\text{Yield}_{\text{fit}}}{\varepsilon \times \mathcal{B}(D^{(*)}) \times N(B^0, \bar{B}^0)}$$

The number of B^0 plus \bar{B}^0 , $N(B^0, \bar{B}^0) = 9.67 \text{ M} \pm 0.10 \text{ M}$, is derived assuming equal branching fractions for charged and neutral B meson decays [10]. The uncertainty in the branching fractions of the $\Upsilon(4S)$ is taken into account in the systematics. The significances of the observed signals in the seven fits is determined from the change in $-2\log\mathcal{L}$ when refit with the signal yield constrained to zero: $\text{significance} = \sqrt{2(\log\mathcal{L} - \log\mathcal{L}_{N_{\text{sig}}=0})}$. We obtain a total significance of 12.1σ for $\bar{B}^0 \rightarrow D^0 \pi^0$ and 5.9σ for $\bar{B}^0 \rightarrow D^{*0} \pi^0$. Varying the PDF shapes within the systematic errors to obtain the lowest signal yield, the statistical significance is reduced to 9.4σ ($\bar{B}^0 \rightarrow D^0 \pi^0$) and 4.2σ ($\bar{B}^0 \rightarrow D^{*0} \pi^0$). We obtain branching fractions of $\mathcal{B}(\bar{B}^0 \rightarrow D^0 \pi^0) = (2.74_{-0.32}^{+0.36} \pm 0.55) \times 10^{-4}$ and $\mathcal{B}(\bar{B}^0 \rightarrow D^{*0} \pi^0) = (2.20_{-0.52}^{+0.59} \pm 0.79) \times 10^{-4}$. The first error is statistical and the second error systematic. Our result for $\bar{B}^0 \rightarrow D^0 \pi^0$ is higher than the previous CLEO upper limit [4]. We ascribe this disagreement, which is of the order of 3.1σ , partly to a statistical fluctuation and partly to the description of the ΔE -background in the old CLEO publication.

We consider sources of systematic uncertainties from the PDF shapes, D and $\Upsilon(4S)$ branching ratios, luminosity, possible fit bias, B candidate reconstruction and cross-feed between different modes. The dominant systematic uncertainty comes from the PDF shapes. The systematic uncertainty on the shapes is derived by varying the PDF shapes within the statistical errors of the fit parametrization as well as comparing the CLEO data in the ΔE and M_B sideband regions to the PDF shapes and taking differences as systematic errors. Figures

¹The parameters of the empirical shapes for $B\bar{B}$ and Continuum background are different.

2 and 3 show our results for $\overline{B}^0 \rightarrow D^{(*)0} \pi^0$ with the number of signal, $B\overline{B}$ and Continuum background as free parameters of the fit. The fit result is projected into a signal region, defined in the $M_B - \Delta E$ plane as $-0.05 < \Delta E < 0.05$ GeV, $5.275 < M_B < 5.285$ GeV. The fit results describe the data well. The background in the sidebands is also well modeled by the fit.

	Mode	Fit Yield (Events)	Signifi- cance(σ)	ϵ (%)	$\mathcal{B}(D^{(*)})$ (%)	$\mathcal{B}(D^{(*)0}\pi^0)$ (10^{-4})
$\overline{B}^0 \rightarrow D^0 \pi^0$	$D^0 \rightarrow K^- \pi^+$	$37.5^{+7.2}_{-6.9}$	8.5	37.1	3.82	2.74 ± 0.53
	$D^0 \rightarrow K^- \pi^+ \pi^0$	$42.1^{+9.0}_{-8.6}$	6.8	13.5	12.94	2.49 ± 0.53
	$D^0 \rightarrow K^- (3\pi)^+$	$44.6^{+10.7}_{-10.2}$	5.3	19.0	7.48	3.25 ± 0.78
Averaged $\mathcal{B}(\overline{B}^0 \rightarrow D^0 \pi^0)$			12.1			$2.74^{+0.36}_{-0.32}$
$\overline{B}^0 \rightarrow D^{*0} \pi^0$	$D^{*0} \rightarrow D^0 \pi^0, D^0 \rightarrow K^- \pi^+$	$6.8^{+3.2}_{-2.8}$	2.4	15.3	2.36	1.95 ± 0.91
	$D^{*0} \rightarrow D^0 \pi^0, D^0 \rightarrow K^- \pi^+ \pi^0$	$7.3^{+4.0}_{-3.6}$	2.8	5.5	8.01	1.72 ± 0.94
	$D^{*0} \rightarrow D^0 \pi^0, D^0 \rightarrow K^- (3\pi)^+$	$8.0^{+4.2}_{-3.7}$	3.1	8.1	4.63	2.21 ± 1.15
	$D^{*0} \rightarrow D^0 \gamma, D^0 \rightarrow K^- \pi^+$	$6.4^{+3.0}_{-2.7}$	3.4	11.4	1.46	3.99 ± 1.89
Averaged $\mathcal{B}(\overline{B}^0 \rightarrow D^{*0} \pi^0)$			5.9			$2.20^{+0.59}_{-0.52}$

TABLE I. Fit yields for all decay modes. Our results are based on the D branching ratios given in column 5 [11]. Our measurement of the B branching ratios is given in the last column.

The observation of $\overline{B}^0 \rightarrow D^{(*)0} \pi^0$ completes the measurement of $D^{(*)} \pi$ final states. This allows us to calculate the relative phase between the isospin 1/2 and 3/2 amplitudes in the $D^{(*)} \pi$ system. The basic relation can be expressed in an amplitude triangle: $\mathcal{A}(\overline{D}^0 \pi^+) = \mathcal{A}(D^- \pi^+) + \sqrt{2} \mathcal{A}(\overline{D}^0 \pi^0)$, following the formulation in [3]. With the PDG values [11] $\mathcal{B}(\overline{D}^0 \pi^+) = (53 \pm 5) \times 10^{-4}$, $\mathcal{B}(D^- \pi^+) = (30 \pm 4) \times 10^{-4}$, $\mathcal{B}(\overline{D}^{*0} \pi^+) = (46 \pm 4) \times 10^{-4}$, $\mathcal{B}(D^{*-} \pi^+) = (27.6 \pm 2.1) \times 10^{-4}$, $\tau(B^+) / \tau(B^0) = 1.073 \pm 0.027$, and our measurement of $\overline{B}^0 \rightarrow D^{(*)0} \pi^0$, we determine the relative phase between the isospin amplitudes to be $\cos \delta_{I,D} = 0.89 \pm 0.08$ for the $D\pi$ final state and $\cos \delta_{I,D^*} = 0.89 \pm 0.08$ for $D^* \pi$. The ratios of isospin amplitudes $A_{1/2} / A_{3/2}$ are 0.70 ± 0.11 ($D\pi$) and 0.74 ± 0.08 ($D^* \pi$). A similar calculation has been performed in [12] using our preliminary results [13] and preliminary results obtained by the Belle collaboration [14].

Models of hadronic B decay [2] have successfully described experimental results using two phenomenological parameters, a_1 and a_2 , that characterize non-factorizable contributions. Both are believed to be process-dependent but so far experimental data have been consistent with universal values for a_1 and a_2 . Recent work by Beneke, Buchalla, Neubert and Sachrajda [15] has shown that a_1 is only slightly process-dependent. Based on our $\overline{B}^0 \rightarrow D^0 \pi^0$ measurement, we derive a value $a_2 = 0.57 \pm 0.06$. Comparing our result to the a_2 value from two-body B decays to charmonium, $a_2 = 0.29$ [2], the process dependence of a_2 is favored [12].

To summarize we observed the color-suppressed decays $\overline{B}^0 \rightarrow D^0 \pi^0$ and $\overline{B}^0 \rightarrow D^{*0} \pi^0$. The number of signal events in our data sample was obtained from an unbinned extended maximum likelihood fit in four variables. The measurements of the two branching fractions are

$\mathcal{B}(\bar{B}^0 \rightarrow D^0 \pi^0) = (2.74_{-0.32}^{+0.36} \pm 0.55) \times 10^{-4}$ and $\mathcal{B}(\bar{B}^0 \rightarrow D^{*0} \pi^0) = (2.20_{-0.52}^{+0.59} \pm 0.79) \times 10^{-4}$. The first error is statistical and the second systematic. The statistical significance of the $D^0 \pi^0$ signal is 12.1σ (5.9σ for $D^{*0} \pi^0$).

We gratefully acknowledge the effort of the CESR staff in providing us with excellent luminosity and running conditions. This work was supported by the National Science Foundation, the U.S. Department of Energy, the Research Corporation and the Texas Advanced Research Program.

REFERENCES

- [1] T. E. Browder, K. Honscheid and D. Pedrini, *Ann. Rev. Nucl. Part. Sci.* **46**, 395 (1996).
- [2] M. Neubert and B. Stech in *Heavy Flavours*, edited by A.J. Buras and M. Lindner (World Scientific, Singapore, 2nd edition 1998).
- [3] J.L. Rosner, *Phys. Rev. D* **60**, 074029 (1999).
- [4] CLEO Collaboration, B. Nemati *et al.*, *Phys. Rev. D* **57**, 5363 (1998).
- [5] CLEO Collaboration, Y. Kubota *et al.*, *Nucl. Instrum. Methods Phys. Res.*, **A320**, 66 (1992).
- [6] T. Hill, *Nucl. Instrum. Methods Phys. Res., Sect. A* **418**, 32 (1998).
- [7] CLEO Collaboration, *Phys. Rev. Lett.* **85**, 515 (2000).
- [8] S.L. Wu, *Phys. Rep. C* **107**, 59 (1984).
- [9] A bifurcated Gaussian is a Gaussian with different widths for the left and right part of the curve.
- [10] CLEO Collaboration, *Phys.Rev.Lett.* **86**, 2737 (2001).
- [11] D.E. Groom *et al.*, (Particle Data Group), *Eur. Phys. Jour.* **C15**, 1 (2000) and 2001 partial update for edition 2002 (URL: <http://pdg.lbl.gov>).
- [12] M. Neubert and A. Petrov, *Phys. Lett.* **B519**, 50 (2001).
- [13] E. von Toerne, in *Proceedings of International Europhysics Conference on High Energy Physics*, Budapest 2001, (to be published).
- [14] R-S. Lu, in *Proceedings of International Europhysics Conference on High Energy Physics*, Budapest, (to be published), and hep-ex/0107048, Final results by the Belle Collaboration: hep-ex/0109021 (to be published).
- [15] M. Beneke *et al.*, *Nucl.Phys.* **B591** (2000) 313.

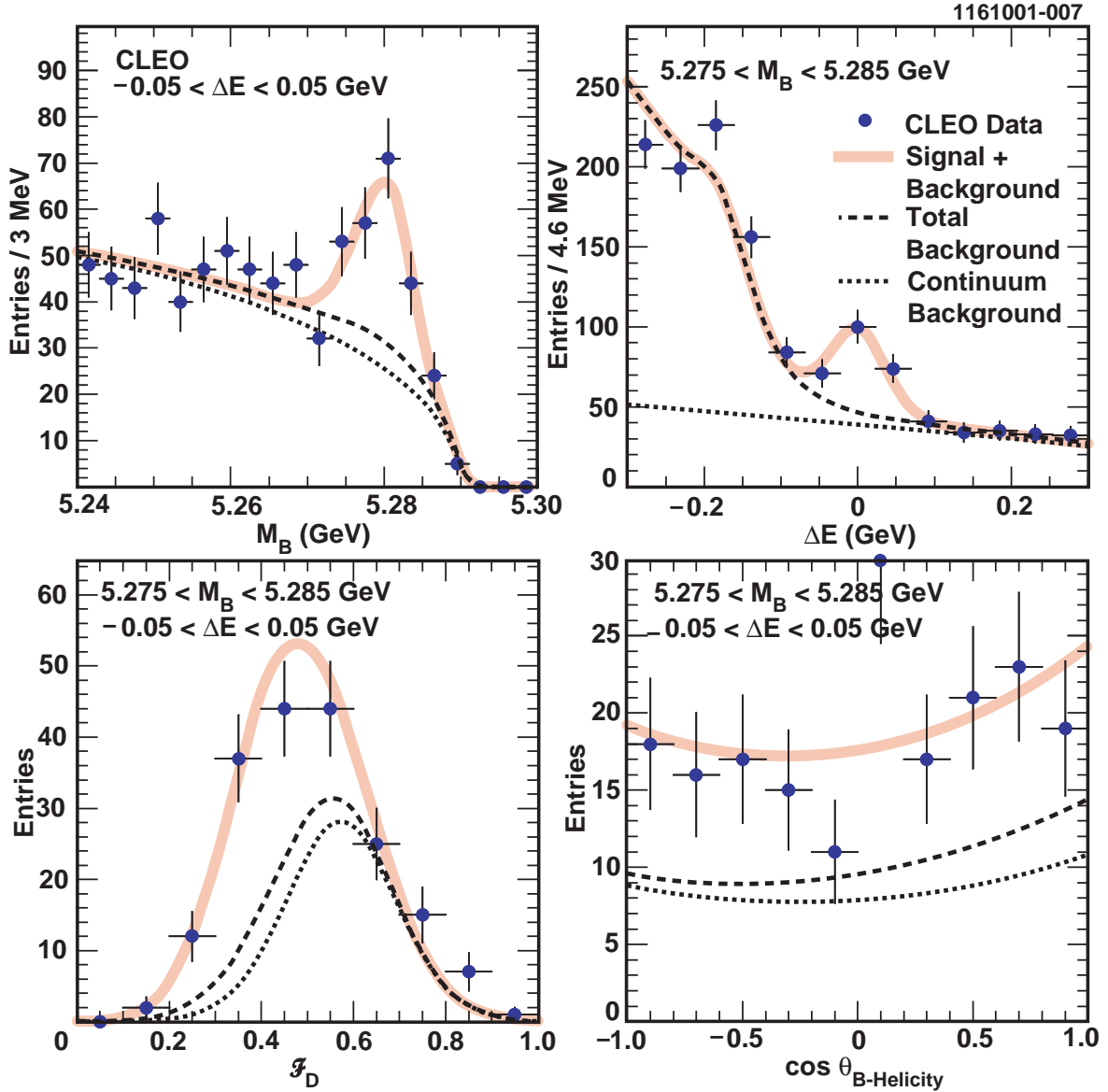


FIG. 2. Distribution of fit input variables for $\bar{B}^0 \rightarrow D^0 \pi^0$. The results of the unbinned, extended maximum likelihood fit are shown as the full line. The dotted line represents the fitted continuum and the dashed line is the fit result for the sum of $B\bar{B}$ and continuum background. To enhance the signal for display purposes, the fit results are projected into the M_B - ΔE signal region $-0.05 < \Delta E < 0.05$ GeV, $5.275 < M_B < 5.285$ GeV.

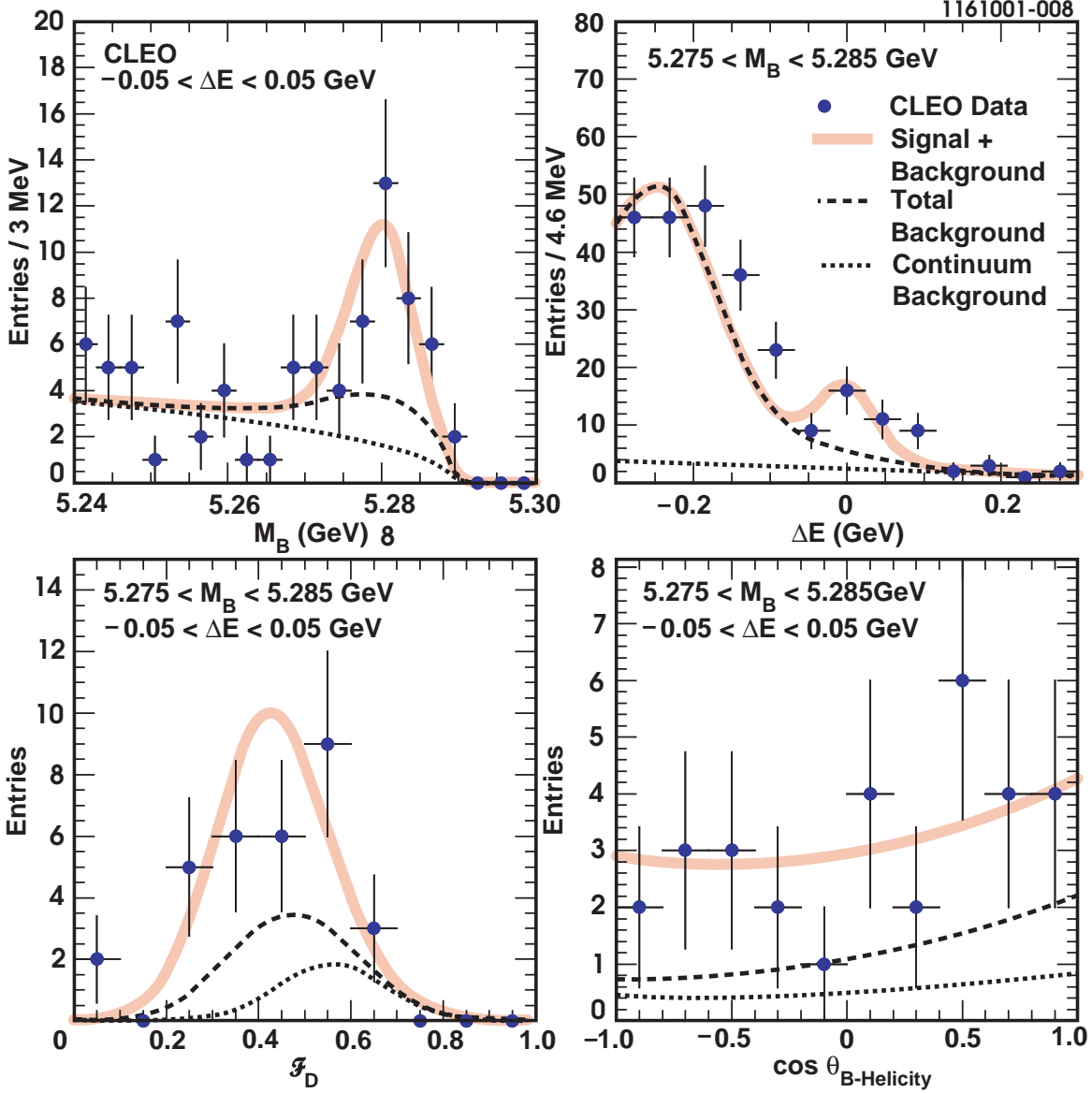


FIG. 3. Distribution of fit input variables for $\overline{B}^0 \rightarrow D^{*0} \pi^0$. The results of the unbinned, extended maximum likelihood fit are shown as the full line. The dotted line represents the fitted continuum and the dashed line is the fit result for the sum of $B\overline{B}$ and continuum background. To enhance the signal for display purposes, the fit results are projected into the M_B - ΔE signal region.